Energy considerations for the stabilization of constrained mechanical systems with velocity projection

Juan C. García orden

Energy considerations for the stabilization of constrained mechanical systems with velocity projection

Juan C. García Orden

Received: date / Accepted: date

Abstract There are many difficulties involved in the numerical integration of index-3 Differential Algebraic Equations (DAEs), mainly related to stability, in the context of mechanical systems. An integrator that exactly enforces the constraint at position level may produce a discrete solution that departs from the velocity and/or acceleration constraint manifolds (invariants). This behaviour affects the stability of the numerical scheme, resulting in the use of stabilization techniques based on enforcing the invariants. A coordinate projection is a poststabilization technique where the solution obtained by a suitable DAE integrator is forced back to the invariant manifolds. This paper analyzes the energy balance of a velocity projection, providing an alternative interpretation of its effect on the stability and a practical criterion for the projection matrix selection.

Keywords time integration, nonlinear dynamics, Differential Algebraic Equation (DAE), poststabilization, velocity projection, energy balance

1 Introduction

Many engineering applications involve the dynamics of several bodies, rigid or deformable, undergoing large motions. Very often the motion of these systems is constrained, because there are joints than connect the different parts, or due to prescribed displacements imposed by the environment.

J.C. García Orden
ETSI Caminos, Canales y Puertos. Universidad Politécnica de Madrid. C/ Profesor Aranguren s/n, 28040 Madrid, Spain
Tel.: +34-91-3365394
Fax: +34-91-3367702
E-mail: juancarlos.garcia@upm.es

The mathematical models associated with these type of systems are typically formulated in terms of index-3 Differential Algebraic Equation (DAE) systems, composed of a set of differential equations, plus a set of algebraic constraint equations expressing additional relations among the generalized coordinates of the model. The numerical solution of these systems poses several difficulties, mostly related to the stability of the available integration schemes.

Direct integration of DAEs with an index higher than one is usually not performed due to stability problems [8], although there have been some recent successful applications based on a second order generalized-α method applied to index-2 and index-3 DAEs (see [2] and references therein). On the other hand, index reduction through the analytical differentiation of the constraint equations causes the progressive drift of the computed solution from the position, velocity or acceleration constraint manifolds (which are invariants of the system) during the simulation. This is the point of departure of several stabilization methods found in the literature [4,3,6].

A coordinate projection is a poststabilization technique based on the solution of a constraint minimization problem, enforcing the solution obtained from the integrator back to the invariant's manifold. This technique has been studied and successfully applied to practical mechanical models by several researchers [12,22,1,13, 20,5,7,9,10]. A detailed analysis and a discussion of the applicability of this technique can be found in the references and is beyond the scope of this paper. Nevertheless, two relevant aspects, related to the performance of this technique as applied to mechanical problems, are not found in the literature.

The first aspect is the relationship between the projection and the mechanical energy balance. It is desir-

able, from a physical point of view, for the behaviour of the energy of the numerical solution to be consistent with the energy of the continuous model. But this aspect is important also from the algorithmic point of view, due to the close relationship between the behaviour of the discrete energy computed by a numerical scheme and its stability [24].

The second aspect is the selection of the projection matrix. [13] proposes an orthogonal projection on the null-space of the invariant, while in [22,1,7,9] a mass-orthogonal projection is employed, and tested in several examples with very good results. References [10, 11] propose a projection based on the mass matrix plus other terms related to the linearized damping and elastic forces of the system, which is numerically more efficient. In fact, from a purely mathematical point of view, any positive definite matrix qualifies for a coordinate projection, which justifies the interest in searching for a practical criterion for selecting the projection matrix.

This paper focuses on these two aspects, analyzing first the energy balance involved in a coordinate projection on velocities. The results of this analysis provide an alternative interpretation of the performance of the technique, leading to a practical criterion for the matrix selection.

2 Constrained dynamics formulation

The point of departure is the formulation of the dynamics of a mechanical system with a configuration defined by the set of generalized coordinates $\mathbf{q} \in \mathbb{R}^n$, under the action of applied forces $\mathbf{f}(\mathbf{q}, \dot{\mathbf{q}}, t)$ and subjected to a set of r holonomic constraints $\mathbf{\Phi} : \mathbb{R}^n \times [0, T] \to \mathbb{R}^r$, such that $\mathbf{\Phi}(\mathbf{q}, t) = \mathbf{0}$.

The *Lagrange multiplier method* leads to an index-3 DAE system given by:

$$\mathbf{M}\ddot{\mathbf{q}} + \mathbf{\Phi}_{\mathbf{q}}^{\mathrm{T}}\boldsymbol{\lambda} = \mathbf{Q} \quad , \quad \mathbf{\Phi} = \mathbf{0} \quad , \tag{1}$$

$\mathbf{M}$ being the mass matrix, $\boldsymbol{\lambda} \in \mathbb{R}^r$ the vector of Lagrange multipliers, and denoted by $(\,)_{\mathbf{q}} \stackrel{\text{def}}{=} \partial(\,)/\partial\mathbf{q}$ and $\dot{(\,)} \stackrel{\text{def}}{=} \mathrm{d}(\,)/\mathrm{d}t$. The vector of generalized forces $\mathbf{Q}(\mathbf{q}, \dot{\mathbf{q}}, t)$ accounts for the applied forces $\mathbf{f}$ and additional terms (gyroscopic, etc.) that may appear due to the particular type of generalized coordinates. If $\mathbf{q}$ are Cartesian coordinates of selected points of the system, these additional terms vanish and $\mathbf{Q} = \mathbf{f}$.

An exact integration of the index-3 DAE system (1) in its original form (meaning that no index reduction is performed) would provide a solution that exactly satisfies the constraint at position level ($\mathbf{\Phi} = \mathbf{0}$). In this case, the constraints at velocity and acceleration levels would also be automatically exactly enforced. This means that a computed solution $\mathbf{q}(t)$ would automatically verify $\dot{\mathbf{\Phi}} = \ddot{\mathbf{\Phi}} = \mathbf{0}$, with no further considerations; we call these *invariants* of the system.

But this situation does not hold in general for the direct numerical solution due to the approximations introduced into the computations. This means that, even though the computed solution satisfies the constraint at position level in a numerical sense (meaning that its error is below the machine precision), the solution may significantly violate the constraint at velocity and acceleration levels.

A similar situation arises when the index of the DAE system (1) is reduced by means of a double differentiation of the constraint equation, leading to the (underlying) ODE system. In this case, the numerical integration provides a solution that satisfies the constraint at acceleration level ($\ddot{\mathbf{\Phi}} = \mathbf{0}$), but progressively violates the constraints at position and velocity levels.

These facts justify the search for algorithms that force the numerical solution to remain on all the invariant's manifolds. This is the point of departure of different stabilization methods proposed in the literature; one of them is a particular poststabilization technique known as *coordinate projection*.

3 Coordinate projection

With this technique, a time-stepping method is applied to (1) in order to obtain a solution for each time step, followed by a projection to bring the solution back to the invariant manifold.

In the case of a *velocity projection*, the velocities $\dot{\mathbf{q}}^*$ computed with the integrator are projected onto the velocity constraint manifold to obtain new velocities $\dot{\mathbf{q}}$, solving a constrained minimization problem given by:

$$\min_{\dot{\mathbf{q}}} \frac{1}{2}(\dot{\mathbf{q}}-\dot{\mathbf{q}}^*)^{\mathrm{T}}\mathbf{A}(\dot{\mathbf{q}}-\dot{\mathbf{q}}^*) \qquad \text{subject to} \quad \dot{\mathbf{\Phi}} = \mathbf{0} \quad , \tag{2}$$

$\mathbf{A}$ being a symmetric and positive definite matrix. This minimization problem can be solved with different methods. For instance, in [22] a Lagrange multiplier method with a Newton-type iteration is employed, while in [7] an augmented-Lagrange method is used. In [10] a penalty method is used with excellent results. In the present paper we choose the same approach, a penalty method, since it allows us to obtain a closed expression for the projected velocities, while performing an efficient projection.

The penalty method transforms the constrained problem (2) into an unconstrained one, introducing a penalty parameter $\alpha > 0$ and leading to an algebraic equation for $\dot{\mathbf{q}}$ given by:

$$\mathbf{A}(\dot{\mathbf{q}} - \dot{\mathbf{q}}^*) + \dot{\mathbf{\Phi}}_{\dot{\mathbf{q}}}^{\mathrm{T}}\alpha\dot{\mathbf{\Phi}} = \mathbf{0} \tag{3}$$

The terms $\dot{\mathbf{\Phi}}$ and $\dot{\mathbf{\Phi}}_{\dot{\mathbf{q}}}$ can be further elaborated as:

$$\dot{\mathbf{\Phi}} = \frac{\partial \mathbf{\Phi}}{\partial \mathbf{q}}\dot{\mathbf{q}} + \frac{\partial \mathbf{\Phi}}{\partial t} = \mathbf{\Phi_q}\dot{\mathbf{q}} + \mathbf{\Phi}_t \qquad ; \qquad \dot{\mathbf{\Phi}}_{\dot{\mathbf{q}}} = \frac{\partial \dot{\mathbf{\Phi}}}{\partial \dot{\mathbf{q}}} = \mathbf{\Phi_q} \, .$$

And assuming that the constraint does not explicitly depend on time ($\mathbf{\Phi}_t = \mathbf{0}$), from (3) the following linear algebraic system for the unknown $\dot{\mathbf{q}}$ is obtained:

$$\left(\mathbf{A} + \alpha \mathbf{\Phi_q}^{\mathrm{T}} \mathbf{\Phi_q}\right) \dot{\mathbf{q}} = \mathbf{A}\dot{\mathbf{q}}^* \tag{4}$$

Remark 1 The fact that the projection matrix $\mathbf{A}$ is positive definite and $\alpha > 0$ guarantees that the linear system given by (4) is non-singular, which means that the projected velocities $\dot{\mathbf{q}}$ are always computable. In order to justify this proposition, it is only necessary to employ some standard linear algebra results, which will be used here without further proof. Recalling that $\mathbf{A}$ is positive definite and using the fact that $\mathbf{\Phi_q}^{\mathrm{T}}\mathbf{\Phi_q}$ is positive semidefinite, the following relation holds for all $\mathbf{x} \neq \mathbf{0}$:

$$\mathbf{x}^{\mathrm{T}} \left(\mathbf{A} + \alpha \mathbf{\Phi_q}^{\mathrm{T}} \mathbf{\Phi_q}\right) \mathbf{x} = \underbrace{\mathbf{x}^{\mathrm{T}} \mathbf{A} \mathbf{x}}_{>0} + \alpha \underbrace{\mathbf{x}^{\mathrm{T}} \left(\mathbf{\Phi_q}^{\mathrm{T}} \mathbf{\Phi_q}\right) \mathbf{x}}_{\geq 0} > 0 \; ,$$

which means that matrix $\left(\mathbf{A} + \alpha \mathbf{\Phi_q}^{\mathrm{T}} \mathbf{\Phi_q}\right)$ is positive definite and, as a consequence, it is non-singular.

Note that the use of the penalty method to solve the minimization problem (2) is approximate, in the sense that, in general, the projected velocities $\dot{\mathbf{q}}$ do not exactly lie on the velocity constraint manifold $\dot{\mathbf{\Phi}}$. In fact, it can be shown that, if a projected velocity $\dot{\mathbf{q}}$ satisfies the velocity constraint, it is because the original velocity $\dot{\mathbf{q}}^\star$ already satisfied this constraint. This assertion is justified in the following proposition.

Proposition 1 *If the velocity before projection ($\dot{\mathbf{q}}^\star$) or the velocity after projection ($\dot{\mathbf{q}}$) satisfies the velocity constraint $\dot{\mathbf{\Phi}} = \mathbf{0}$, then $\dot{\mathbf{q}}^* = \dot{\mathbf{q}}$.*

In order to prove this proposition, let us consider first a compatible projected velocity $\dot{\mathbf{q}}$, verifying $\dot{\mathbf{\Phi}} = \mathbf{\Phi_q}\dot{\mathbf{q}} = \mathbf{0}$. Introducing this result into (4) and taking into account that the projection matrix $\mathbf{A}$ is definite, it immediately follows that:

$$\mathbf{A}\dot{\mathbf{q}} + \alpha \mathbf{\Phi_q}^{\mathrm{T}} \underbrace{\mathbf{\Phi_q}\dot{\mathbf{q}}}_{\mathbf{0}} = \mathbf{A}\dot{\mathbf{q}}^* \quad \Longrightarrow \quad \dot{\mathbf{q}} = \dot{\mathbf{q}}^*$$

On the other hand, let us now consider a compatible original velocity $\dot{\mathbf{q}}^*$, verifying $\dot{\mathbf{\Phi}} = \mathbf{\Phi_q}\dot{\mathbf{q}}^* = \mathbf{0}$. Again using equation (4), and premultiplying it by $(\dot{\mathbf{q}} - \dot{\mathbf{q}}^*)^{\mathrm{T}}$, the following relations are obtained:

$$\begin{aligned} \left(\mathbf{A} + \alpha \mathbf{\Phi_q}^{\mathrm{T}} \mathbf{\Phi_q}\right) \dot{\mathbf{q}} &= \mathbf{A}\dot{\mathbf{q}}^* \\ \mathbf{A}\left(\dot{\mathbf{q}} - \dot{\mathbf{q}}^*\right) + \alpha \mathbf{\Phi_q}^{\mathrm{T}} \mathbf{\Phi_q}\dot{\mathbf{q}} &= \mathbf{0} \\ \left(\dot{\mathbf{q}} - \dot{\mathbf{q}}^*\right)^{\mathrm{T}} \mathbf{A} \left(\dot{\mathbf{q}} - \dot{\mathbf{q}}^*\right) + \alpha \left(\dot{\mathbf{q}} - \dot{\mathbf{q}}^*\right)^{\mathrm{T}} \mathbf{\Phi_q}^{\mathrm{T}} \mathbf{\Phi_q}\dot{\mathbf{q}} &= 0 \end{aligned} \tag{5}$$

The first term in equation (5) is positive for $\dot{\mathbf{q}} \neq \dot{\mathbf{q}}^*$, since projection matrix $\mathbf{A}$ is positive definite. The second term of (5) can be further elaborated as:

$$\begin{aligned} \alpha \dot{\mathbf{q}}^{\mathrm{T}} \mathbf{\Phi_q}^{\mathrm{T}} \mathbf{\Phi_q}\dot{\mathbf{q}} - \alpha \dot{\mathbf{q}}^{*^{\mathrm{T}}} \mathbf{\Phi_q}^{\mathrm{T}} \mathbf{\Phi_q}\dot{\mathbf{q}} = \\ = \alpha \underbrace{\dot{\mathbf{q}}^{\mathrm{T}} \mathbf{\Phi_q}^{\mathrm{T}} \mathbf{\Phi_q}\dot{\mathbf{q}}}_{\geq 0} - \alpha \underbrace{\left(\mathbf{\Phi_q}\dot{\mathbf{q}}^*\right)^{\mathrm{T}}}_{=\mathbf{0}} \mathbf{\Phi_q}\dot{\mathbf{q}} \; \geq 0 \end{aligned}$$

Taking into account the previous results, it becomes apparent that the only $\dot{\mathbf{q}}$ that satisfies equation (5) is $\dot{\mathbf{q}} = \dot{\mathbf{q}}^*$, which concludes our proving of the proposition. □

Projections can also be performed at the position and acceleration levels. For instance, in the case of an *acceleration projection*, the accelerations computed with the ODE integrator ($\ddot{\mathbf{q}}^*$) are projected onto the acceleration constraint manifold to obtain new accelerations ($\ddot{\mathbf{q}}$), solving a constrained minimization problem given by:

$$\min_{\ddot{\mathbf{q}}} \frac{1}{2}(\ddot{\mathbf{q}} - \ddot{\mathbf{q}}^*)^{\mathrm{T}} \mathbf{A} (\ddot{\mathbf{q}} - \ddot{\mathbf{q}}^*) \qquad \text{subject to} \quad \ddot{\mathbf{\Phi}} = \mathbf{0} \quad , \tag{6}$$

$\mathbf{A}$ being a positive definite matrix.[1] Again, this constrained minimization problem can be solved with penalty, which leads to the solution for $\ddot{\mathbf{q}}$ as a linear algebraic system given by:

$$\left(\mathbf{A} + \alpha \mathbf{\Phi_q}^{\mathrm{T}} \mathbf{\Phi_q}\right) \ddot{\mathbf{q}} = \mathbf{A}\ddot{\mathbf{q}}^* - \alpha \mathbf{\Phi_q}^{\mathrm{T}} \dot{\mathbf{\Phi}}_{\mathbf{q}} \dot{\mathbf{q}} \tag{7}$$

The analysis of position and acceleration projections is outside the scope of this paper, and only a *velocity projection* will be considered. This is justified by the results reported in [22,1,20]. These authors show that errors in the velocity constraint are more critical for the numerical solution than errors in the position constraint, coming to the conclusion that velocity projection is the most efficient projection for improving numerical integration.

4 Total energy balance

For systems of ODEs arising from the dynamics of mechanical systems, the stability of the numerical methods used to solve them is often related to the concept of energy. Actually, in the linear case, exact algorithmic energy conservation leads to unconditional stability, as happens, for instance, with the trapezoidal rule [21]. However, this direct relationship does not hold for the nonlinear case [23,24], which is the case of the equations

[1] not necessarily the same employed for the velocity projection

resulting from practical multibody systems. Nevertheless, exact conservation of energy (or unconditional energy dissipation) has revealed itself to be extremely useful in the design of robust integration schemes, with excellent stability in the nonlinear case ([24] and references therein) and applied to the dynamics of multibody systems [14,18,15,16].

With these arguments in mind, it is interesting to analyze how the coordinate projection behaves in terms of energy balance. As will be shown below, it turns out that the projection actually controls the energy, therefore providing a new point of view for the understanding of its stabilization properties.

In order to establish a suitable point of departure, let us consider a constrained mechanical system, represented by a set of coordinates $\mathbf{q} \in \mathbb{R}^n$, subjected to a set of r holonomic constraints $\mathbf{\Phi}(\mathbf{q}) \in \mathbb{R}^r$ and without applied forces. The dynamics of this system are represented by the index-3 DAE:

$$\mathbf{M}\ddot{\mathbf{q}} + \mathbf{Q}_{\mathbf{\Phi}}(\mathbf{q}) = \mathbf{Q} \quad , \qquad \mathbf{\Phi} = \mathbf{0} \tag{8}$$

$\mathbf{Q}_{\mathbf{\Phi}}$ being the constraint force vector, which in the case of the Lagrange multiplier method is given by $\mathbf{Q}_{\mathbf{\Phi}} = \mathbf{\Phi}_{\mathbf{q}}^{\mathrm{T}}\boldsymbol{\lambda}$. The generalized force vector $\mathbf{Q}$ vanishes if $\mathbf{q}$ contains Cartesian coordinates of selected points of the system.

Remark 2 The fact that no applied forces (e.g. external loads or internal forces in discretized deformable bodies) are considered in (8) does not limit the applicability of the developments presented in the next sections. This is due to the fact that the velocity projection does not affect the work performed by these forces, which typically depends only on positions.

Remark 3 The dynamical system represented by (8) is conservative (the total mechanical energy remains constant), since the work performed by the holonomic constraints which do not depend explicitly on time is zero.

Directly integrating the index-3 DAE (8) from t_n to t_{n+1} provides a solution $\mathbf{q}_{n+1}$ that exactly satisfies the position constraint. In consequence, the constraint force at t_{n+1} takes the value $\mathbf{Q}_{\mathbf{\Phi}_{n+1}} = \mathbf{\Phi}_{\mathbf{q}_{n+1}}^{\mathrm{T}}\boldsymbol{\lambda}_{n+1}$, $\boldsymbol{\lambda}_{n+1}$ being the vector of exact Lagrange multipliers.

A velocity vector $\dot{\mathbf{q}}_{n+1}^{*}$ is also obtained, but in general, the velocity constraint $\dot{\mathbf{\Phi}}_{n+1}$ is not exactly satisfied. In order to move the solution back to the velocity constraint manifold, let us assume that a velocity projection is performed at the end of each time step as explained in section 3, obtaining a new velocity vector $\dot{\mathbf{q}}_{n+1}$.

The total discrete energy balance ΔE between t_n and t_{n+1} is given by:

$$\Delta E = \frac{1}{2}\dot{\mathbf{q}}_{n+1}^{\mathrm{T}}\mathbf{M}\dot{\mathbf{q}}_{n+1} - \frac{1}{2}\dot{\mathbf{q}}_{n}^{\mathrm{T}}\mathbf{M}\dot{\mathbf{q}}_{n} \tag{9}$$

Note that the energy balance ΔE given by (9) equals the kinetic energy balance. This is due to the fact that there are no applied forces, the position constraints are exactly satisfied, and the position $\mathbf{q}_{n+1}$ does not change under the projection.

Adding and subtracting a term $(1/2)\dot{\mathbf{q}}_{n+1}^{*^{\mathrm{T}}}\mathbf{M}\dot{\mathbf{q}}_{n+1}^{*}$ in equation (9), the following relation is obtained:

$$\Delta E = \underbrace{\frac{1}{2}\dot{\mathbf{q}}_{n+1}^{*^{\mathrm{T}}}\mathbf{M}\dot{\mathbf{q}}_{n+1}^{*} - \frac{1}{2}\dot{\mathbf{q}}_{n}^{\mathrm{T}}\mathbf{M}\dot{\mathbf{q}}_{n}}_{\Delta E_i} + \underbrace{\frac{1}{2}\dot{\mathbf{q}}_{n+1}^{\mathrm{T}}\mathbf{M}\dot{\mathbf{q}}_{n+1} - \frac{1}{2}\dot{\mathbf{q}}_{n+1}^{*^{\mathrm{T}}}\mathbf{M}\dot{\mathbf{q}}_{n+1}^{*}}_{\Delta E_p} \quad , \tag{10}$$

ΔE_i being the energy variation introduced by the ODE integrator, and ΔE_p the energy variation introduced by the velocity projection.

It is not difficult to obtain an expression for the energy variation ΔE_i introduced by a standard ODE integrator. The point of departure is the first term of (10) rewritten as:

$$\Delta E_i = \frac{1}{2}(\dot{\mathbf{q}}_{n+1}^{*} + \dot{\mathbf{q}}_{n})^{\mathrm{T}}\mathbf{M}(\dot{\mathbf{q}}_{n+1}^{*} - \dot{\mathbf{q}}_{n}) \tag{11}$$

and using the algorithmic expressions of the method with the original system (8). For instance, for the *trapezoidal rule* the following relations hold:

$$\dot{\mathbf{q}}_{n+1}^{*} + \dot{\mathbf{q}}_{n} = \frac{2}{\Delta t}(\mathbf{q}_{n+1} - \mathbf{q}_{n})$$
$$\dot{\mathbf{q}}_{n+1}^{*} - \dot{\mathbf{q}}_{n} = -\frac{\Delta t}{2}\mathbf{M}^{-1}\left(\mathbf{Q}_{\mathrm{T}_n} + \mathbf{Q}_{\mathrm{T}_{n+1}}\right)$$

with $\mathbf{Q}_{\mathrm{T}} = \mathbf{Q}_{\mathbf{\Phi}} - \mathbf{Q}$, which introduced into expression (11) give, after some algebra:

$$\Delta E_i = -(\mathbf{q}_{n+1} - \mathbf{q}_{n})^{\mathrm{T}}\ \overline{\mathbf{Q}}_{\mathrm{T}_{n+\frac{1}{2}}} \ , \tag{12}$$

where the notation $\overline{(\cdot)}_{n+\frac{1}{2}} \stackrel{\text{def}}{=} \left[(\cdot)_n + (\cdot)_{n+1}\right]/2.$ has been employed.

Another example is the *implicit midpoint rule*, which introduces an energy variation given by:

$$\Delta E_i = -(\mathbf{q}_{n+1} - \mathbf{q}_{n})^{\mathrm{T}}\ \mathbf{Q}_{\mathrm{T}_{n+\frac{1}{2}}} \tag{13}$$

where $(\cdot)_{n+\frac{1}{2}}$ denotes evaluation at the midpoint. Note that, in a general nonlinear case, $\overline{\mathbf{Q}}_{\mathrm{T}_{n+\frac{1}{2}}} \neq \mathbf{Q}_{\mathrm{T}_{n+\frac{1}{2}}}$ and $\Delta E_i \neq 0$ can be positive or negative. Note also from (12) and (13) that both numerical schemes are the same and exactly conserve energy ($\Delta E_i = 0$) in the linear case.

Another interesting example is a *conserving algorithm*, which does not introduce artificial energy by means of a specific formulation of the force $\mathbf{Q}_{\mathrm{T}}^{c}$:

$$\Delta E_i = -(\mathbf{q}_{n+1} - \mathbf{q}_n)^{\mathrm{T}} \mathbf{Q}_{\mathrm{T}}^{c} = 0 \tag{14}$$

Details about the formulation of $\mathbf{Q}_{\mathrm{T}}^{c}$ with Cartesian coordinates ($\mathbf{Q}_{\mathrm{T}} = \mathbf{Q}_{\mathbf{\Phi}}$) employing the Lagrange multipliers method and the augmented Lagrange multipliers method can be found in [19] and [17], respectively.

Other expressions similar to (12), (13) and (14) can be obtained for other integrators, but an exhaustive description falls outside the scope of the work presented here. It is important to remark that the sign of the energy contribution ΔE_i may not be constant throughout the simulation, thus increasing or decreasing the total energy, which can in turn affect numerical stability.

The second contribution to the energy variation is ΔE_p, associated with the velocity projection described in section 3, and can be obtained solving a minimization problem with a definite positive matrix $\mathbf{A}$ using a penalty method. This leads to the solution for $\dot{\mathbf{q}}_{n+1}$ of the linear algebraic equation system (4), given by:

$$\dot{\mathbf{q}}_{n+1} = \mathbf{P}^{-1}\, \dot{\mathbf{q}}^{*}_{n+1} \qquad \text{with} \quad \mathbf{P} = \left(\mathbf{1} + \alpha \mathbf{A}^{-1} \mathbf{\Phi}_{\mathbf{q}}^{\mathrm{T}} \mathbf{\Phi}_{\mathbf{q}}\right) \tag{15}$$

Introducing the first expression in (15) in the following relation for ΔE_p:

$$\Delta E_p = \frac{1}{2} (\dot{\mathbf{q}}_{n+1} + \dot{\mathbf{q}}^{*}_{n+1})^{\mathrm{T}} \mathbf{M} (\dot{\mathbf{q}}_{n+1} - \dot{\mathbf{q}}^{*}_{n+1})$$

an expression is obtained for the energy variation introduced in the velocity projection:

$$\Delta E_p = \dot{\mathbf{q}}_{n+1}^{\mathrm{T}} \mathbf{D} \dot{\mathbf{q}}_{n+1} \quad \text{with} \quad \mathbf{D} = \frac{1}{2} \left(\mathbf{1} + \mathbf{P}\right)^{\mathrm{T}} \mathbf{M} \left(\mathbf{1} - \mathbf{P}\right) \tag{16}$$

Therefore, the effect of the projection upon the energy depends of the properties of the matrix $\mathbf{D}$, which is the matrix associated with the quadratic form ΔE_p, and governs the damping behaviour of the projection. If this matrix is negative semidefinite, artificial energy growth is avoided in all cases, and a significant improvement in the stability of the overall numerical scheme would be expected.

In what follows, a detailed analysis of this projection energy balance is performed, which will provide a practical assessment of the suitable choice for projection matrix $\mathbf{A}$, so that artificial energy growth is unconditionally avoided.

5 Projection energy balance

5.1 Some preliminary results

The point of departure is to perform a quick inspection of the basic properties of the damping matrix $\mathbf{D}$ based on its definition (16) and some basic linear algebra results. It follows that matrices $\mathbf{A}^{-1}$ and $\mathbf{\Phi}_{\mathbf{q}}^{\mathrm{T}} \mathbf{\Phi}_{\mathbf{q}}$ are symmetric and positive semidefinite. However, matrix $\mathbf{P}$ defined in (15) is not, in general, positive semidefinite, or even symmetric. As a consequence, the damping matrix $\mathbf{D}$ given by (16) will not be symmetric, and nothing can be said in general about its definiteness. This means that, following this procedure, it is not possible to bring the sign of the energy balance ΔE_p forward at each time step.

Nevertheless, it is possible to get more information about the quadratic form ΔE_p as explained in the following proposition:

Proposition 2 *The quadratic form ΔE_p given by (16) is degenerate,* i.e. *its kernel $\mathcal{K}_{\mathrm{D}}$:*

$$\mathcal{K}_{\mathrm{D}} = \{\mathbf{x} \in \mathbb{R}^n \ ; \ \mathbf{y}^{\mathrm{T}} \mathbf{D} \mathbf{x} = 0, \ \forall \mathbf{y} \in \mathbb{R}^n\} \tag{17}$$

contains other vectors than the zero vector. Specifically, the set $\mathcal{C}$ of velocity vectors which are compatible with the constraint $\dot{\mathbf{\Phi}}$:

$$\mathcal{C} = \{\dot{\mathbf{q}} \in \mathbb{R}^n \ ; \ \dot{\mathbf{\Phi}} = \mathbf{\Phi}_{\mathbf{q}} \dot{\mathbf{q}} = \mathbf{0}\}$$

is a subset of the kernel, thus $\mathcal{C} \subset \mathcal{K}_{\mathrm{D}}$.

To prove this proposition, let us consider a given compatible velocity vector $\dot{\mathbf{q}} \in \mathcal{C}$; using expressions (15) and (16) it follows that:

$$\mathbf{P}\dot{\mathbf{q}} = \dot{\mathbf{q}} + \alpha \mathbf{A}^{-1} \mathbf{\Phi}_{\mathbf{q}}^{\mathrm{T}} \underbrace{\mathbf{\Phi}_{\mathbf{q}} \dot{\mathbf{q}}}_{\mathbf{0}} = \dot{\mathbf{q}}$$

$$\mathbf{D}\dot{\mathbf{q}} = \frac{1}{2} \left(\mathbf{1} + \mathbf{P}\right)^{\mathrm{T}} \mathbf{M} \left(\mathbf{1} - \mathbf{P}\right) \dot{\mathbf{q}}$$

$$= \frac{1}{2} \left(\mathbf{1} + \mathbf{P}\right)^{\mathrm{T}} \mathbf{M} \underbrace{(\dot{\mathbf{q}} - \mathbf{P}\dot{\mathbf{q}})}_{\mathbf{0}} = \mathbf{0}$$

$$\Delta E_p = \mathbf{x}^{\mathrm{T}} \mathbf{D} \dot{\mathbf{q}} = 0 \quad , \quad \forall \mathbf{x} \in \mathbb{R}^n \quad ,$$

which means that the vector $\dot{\mathbf{q}}$ belongs to $\mathcal{K}_{\mathrm{D}}$. □

This result was already expected, recalling from Proposition 1 that projected velocities that are compatible come from compatible original velocities, which means that projection leaves them unchanged. Note also that this result does not exclude the possibility that incompatible velocities may be undamped; in other words, $\mathcal{C}$ may not coincide with $\mathcal{K}_D$. This issue will be discussed again later.

Summarizing, this preliminary inspection reveals that there are few things to say about the damping introduced by the projection with a general definite positive projection matrix $\mathbf{A}$, apart from the expected fact that compatible velocities never introduce artificial energy.

The next step is to try to find a set of requirements such that, if satisfied by the projection matrix $\mathbf{A}$, they would determine the behaviour of the projection energy balance. If achieved, this result would help in the selection of the projection matrix, which is one of the main goals of this paper.

5.2 Conditions for energy dissipation

It is a basic linear algebra result that any quadratic form may always be expressed in terms of a symmetric matrix. This means that, in order to analyze the properties of the quadratic form given by (16), it is possible to work just with the symmetric part of matrix $\mathbf{D}$. Denoting the symmetric and skew-symmetric parts of the original matrix by superscripts s and h, respectively, this result may be expressed as:

$$\mathbf{x}^{\mathrm{T}}\mathbf{D}\mathbf{x} = \mathbf{x}^{\mathrm{T}}\mathbf{D}^{s}\mathbf{x} + \underbrace{\mathbf{x}^{\mathrm{T}}\mathbf{D}^{h}\mathbf{x}}_{\mathbf{0}} \qquad \text{for all } \mathbf{x} \in \mathbb{R}^{n} \quad , \quad (18)$$

where the symmetric matrix $\mathbf{D}^s$ can be expressed, after some algebraic manipulations using definition (16), as:

$$\mathbf{D}^{s} = \frac{1}{2}\left(\mathbf{D} + \mathbf{D}^{\mathrm{T}}\right) = \frac{1}{2}\left(\mathbf{M} - \mathbf{P}^{\mathrm{T}}\mathbf{M}\mathbf{P}\right)$$

Remark 4 Matrices $\mathbf{D}$ and $\mathbf{D}^s$ both have the same definiteness property (definite, semidefinite, etc.), as immediately follows from equation (18); and their associated quadratic forms have the same kernel $\mathcal{K}_{\mathrm{D}} = \mathcal{K}_{\mathrm{D}^s}$.

Matrix $\mathbf{D}^s$ can be further elaborated and written in terms of the projection matrix $\mathbf{A}$ and the Jacobian $\mathbf{\Phi_q}$ using equation (15) for $\mathbf{P}$, obtaining:

$$\mathbf{D}^{s} = -\alpha\left(\mathbf{B}^{s} + \frac{1}{2}\alpha\mathbf{B}^{\mathrm{T}}\mathbf{M}^{-1}\mathbf{B}\right) \quad , \quad (19)$$

$\mathbf{B}$ being a matrix given by:

$$\mathbf{B} = \mathbf{M}\mathbf{A}^{-1}\mathbf{\Phi}_{\mathbf{q}}^{\mathrm{T}}\mathbf{\Phi_q} \quad , \quad (20)$$

and again denoting the symmetric part of the matrix by the superscript s. Based on (19), the energy balance of the projection may be expressed as:

$$\begin{aligned}\Delta E_p = \dot{\mathbf{q}}^{\mathrm{T}}\mathbf{D}^{s}\dot{\mathbf{q}} &= -\alpha\dot{\mathbf{q}}^{\mathrm{T}}\mathbf{B}^{s}\dot{\mathbf{q}} - \frac{1}{2}\alpha^{2}\left(\mathbf{B}\dot{\mathbf{q}}\right)^{\mathrm{T}}\mathbf{M}^{-1}\left(\mathbf{B}\dot{\mathbf{q}}\right) \\ &= \Delta E_{p_1} + \Delta E_{p_2} \quad . \end{aligned} \quad (21)$$

Note that, since the penalty method is employed to solve the minimization problem (2), the projected velocity vector $\dot{\mathbf{q}}$ may be incompatible (meaning that it may not lie exactly over the velocity constraint manifold $\dot{\mathbf{\Phi}}$).

Thus, the projection energy balance is positive or negative depending on the sign of each term ΔE_{p_1} and ΔE_{p_2} in (21) for an incompatible projected velocity $\dot{\mathbf{q}} \notin \mathcal{C}$. (Recall from Proposition 2 that $\Delta E_p = 0$ for a compatible velocity $\dot{\mathbf{q}} \in \mathcal{C}$.)

In order to gain further insight into the sign of the energy balance (21), it is advisable to study the relationships among the kernels of the following mathematical objects:

– The quadratic form ΔE_p, defined by the damping matrix $\mathbf{D}^s$. Its kernel $\mathcal{K}_{\mathrm{D}^s} = \mathcal{K}_{\mathrm{D}}$ was already defined in (17), and contains all velocity vectors $\dot{\mathbf{q}}$ that do not introduce artificial projection energy:

$$\mathcal{K}_{\mathrm{D}} = \mathcal{K}_{\mathrm{D}^s} = \{\mathbf{x} \in \mathbb{R}^{n} \ ; \ \mathbf{y}^{\mathrm{T}}\mathbf{D}\mathbf{x} = 0, \ \forall \mathbf{y} \in \mathbb{R}^{n}\} \quad (22)$$

– The linear function defined by the matrix $\mathbf{\Phi_q}$. Since $\dot{\mathbf{\Phi}} = \mathbf{\Phi_q}\dot{\mathbf{q}}$, its kernel coincides with the set of compatible velocity vectors $\mathcal{C}$:

$$\mathcal{C} = \{\dot{\mathbf{q}} \in \mathbb{R}^{n} \ ; \ \dot{\mathbf{\Phi}} = \mathbf{\Phi_q}\dot{\mathbf{q}} = \mathbf{0}\} \quad (23)$$

– The linear function defined by the matrix $\mathbf{B}$ given by (20), with a kernel $\mathcal{K}_{\mathrm{B}}$ defined by:

$$\mathcal{K}_{\mathrm{B}} = \{\mathbf{x} \in \mathbb{R}^{n} \ ; \ \mathbf{B}\mathbf{x} = \mathbf{0}\} \quad (24)$$

Proposition 3 *Set $\mathcal{C}$ of compatible velocity vectors is a subset of $\mathcal{K}_{\mathrm{B}}$. In addition, if the matrix $(\mathbf{M}\mathbf{A}^{-1})^s$ is definite then $\mathcal{C} = \mathcal{K}_{\mathrm{B}}$.*

In order to prove the first part of the proposition, let us consider a vector $\mathbf{x} \in \mathcal{C}$. Based on the definition of matrix $\mathbf{B}$ given by (20), then:

$$\mathbf{B}\mathbf{x} = \mathbf{M}\mathbf{A}^{-1}\mathbf{\Phi}_{\mathbf{q}}^{\mathrm{T}}\underbrace{\mathbf{\Phi_q}\mathbf{x}}_{\mathbf{0}} = \mathbf{0} \qquad \longrightarrow \qquad \mathbf{x} \in \mathcal{K}_{\mathrm{B}}$$

For the second part of the proposition, let us consider a vector $\mathbf{x} \neq \mathbf{0}$, $\mathbf{x} \in \mathcal{K}_{\mathrm{B}}$. Again, using definition (20) for matrix $\mathbf{B}$, and taking into account that $(\mathbf{M}\mathbf{A}^{-1})^s$ is definite, the following relations hold:

$$\begin{aligned} \mathbf{B}\mathbf{x} &= \mathbf{0} \\ (\mathbf{M}\mathbf{A}^{-1})\mathbf{\Phi}_{\mathbf{q}}^{\mathrm{T}}\mathbf{\Phi_q}\mathbf{x} &= \mathbf{0} \\ \left(\mathbf{\Phi}_{\mathbf{q}}^{\mathrm{T}}\mathbf{\Phi_q}\mathbf{x}\right)^{\mathrm{T}}(\mathbf{M}\mathbf{A}^{-1})^{s}\mathbf{\Phi}_{\mathbf{q}}^{\mathrm{T}}\mathbf{\Phi_q}\mathbf{x} = 0 \ &\longrightarrow \ (\mathbf{\Phi}_{\mathbf{q}}^{\mathrm{T}}\mathbf{\Phi_q})\mathbf{x} = \mathbf{0} \end{aligned}$$

Pre-multiplying the last relation by vector $\mathbf{x}^{\mathrm{T}}$, it follows that:

$$\mathbf{x}^{\mathrm{T}}(\mathbf{\Phi}_{\mathbf{q}}^{\mathrm{T}}\mathbf{\Phi_q})\mathbf{x} = 0 = (\mathbf{\Phi_q}\mathbf{x})^{\mathrm{T}}(\mathbf{\Phi_q}\mathbf{x}) \quad \longrightarrow \quad \mathbf{\Phi_q}\mathbf{x} = \mathbf{0}$$

which means that $\mathbf{x} \in \mathcal{C}$, and finally implies that $\mathcal{C} = \mathcal{K}_{\mathrm{B}}$. □

Proposition 4 *Set $\mathcal{K}_{\mathrm{B}}$ is a subset of the set of velocity vectors that do not introduce artificial energy, $\mathcal{K}_{\mathrm{D}}$. Besides, if $\mathbf{B}^s$ is positive semidefinite, then $\mathcal{K}_{\mathrm{B}} = \mathcal{K}_D$.*

Again, in order to prove the first part of the proposition, let us consider a vector $\mathbf{x} \in \mathcal{K}_{\mathrm{B}}$. Based on the definition of matrix $\mathbf{D}^s$ given by (19), then:

$$\mathbf{x}^{\mathrm{T}}\mathbf{D}^s\mathbf{x} = -\alpha \underbrace{\mathbf{x}^{\mathrm{T}}\mathbf{B}^s\mathbf{x}}_{=\mathbf{x}^{\mathrm{T}}\mathbf{B}\mathbf{x}=0} - \frac{1}{2}\alpha^2\mathbf{x}^{\mathrm{T}}\mathbf{B}^{\mathrm{T}}\mathbf{M}^{-1}\underbrace{\mathbf{B}\mathbf{x}}_{\mathbf{0}} = 0$$
$$\longrightarrow \quad \mathbf{x} \in \mathcal{K}_{\mathrm{D}}$$

For the second part of the proposition, let us consider a vector $\mathbf{x} \in \mathcal{K}_{\mathrm{D}^s}$. Again, using definition (19) for the matrix $\mathbf{D}^s$ it follows that:

$$\mathbf{x}^{\mathrm{T}}\mathbf{D}^s\mathbf{x} = -\alpha\mathbf{x}^{\mathrm{T}}\mathbf{B}^s\mathbf{x} - \frac{1}{2}\alpha^2\mathbf{x}^{\mathrm{T}}\mathbf{B}^{\mathrm{T}}\mathbf{M}^{-1}\mathbf{B}\mathbf{x} = 0 \qquad (25)$$

If the matrix $\mathbf{B}^s$ is positive semidefinite, then the first term of (25) verifies:

$$\mathbf{x}^{\mathrm{T}}\mathbf{B}^s\mathbf{x} = \mathbf{x}^{\mathrm{T}}\mathbf{B}\mathbf{x} \geq 0 \quad , \qquad \forall \mathbf{x} \neq \mathbf{0} \qquad (26)$$

What is more, since $\mathbf{M}^{-1}$ is positive definite, the second term of (25) verifies:

$$\mathbf{x}^{\mathrm{T}}\mathbf{B}^{\mathrm{T}}\mathbf{M}^{-1}\mathbf{B}\mathbf{x} = (\mathbf{B}\mathbf{x})^{\mathrm{T}}\,\mathbf{M}^{-1}(\mathbf{B}\mathbf{x}) > 0 \ , \quad \forall (\mathbf{B}\mathbf{x}) \neq \mathbf{0} \qquad (27)$$

From (25), (26) and (27) it follows that $\mathbf{B}\mathbf{x} = \mathbf{0}$, which means that $\mathbf{x} \in \mathcal{K}_{\mathrm{B}}$, leading finally to $\mathcal{K}_{\mathrm{B}} = \mathcal{K}_{\mathrm{D}}$. □

Based on Propositions 3 and 4 above, the following proposition may be immediately stated without further proof, and it is illustrated in Figure 1:

Proposition 5 *The following relation holds for the kernels defined by (22), (23) and (24):*

$$\mathcal{C} \subseteq \mathcal{K}_B \subseteq \mathcal{K}_D$$

If matrix $(\mathbf{M}\mathbf{A}^{-1})^s$ is definite, then $\mathcal{C} = \mathcal{K}_{\mathrm{B}}$. If matrix $\mathbf{B}^s$ is positive semidefinite, then $\mathcal{K}_{\mathrm{B}} = \mathcal{K}_D$.

Based on Proposition 5, it is possible to go back now to the expression of the projection energy balance (21) and engage in a more detailed discussion about its sign.

Different situations may arise, depending on the compatibility of a projected velocity $\dot{\mathbf{q}} \neq \mathbf{0}$:

1. If $\dot{\mathbf{q}}$ is compatible, it also lies in the kernel of the projection energy. As a consequence, artificial energy is not introduced ($\Delta E_p = 0$).
2. If $\dot{\mathbf{q}}$ is incompatible, but still lies inside the kernel of the projection energy, artificial energy is not introduced ($\Delta E_p = 0$).

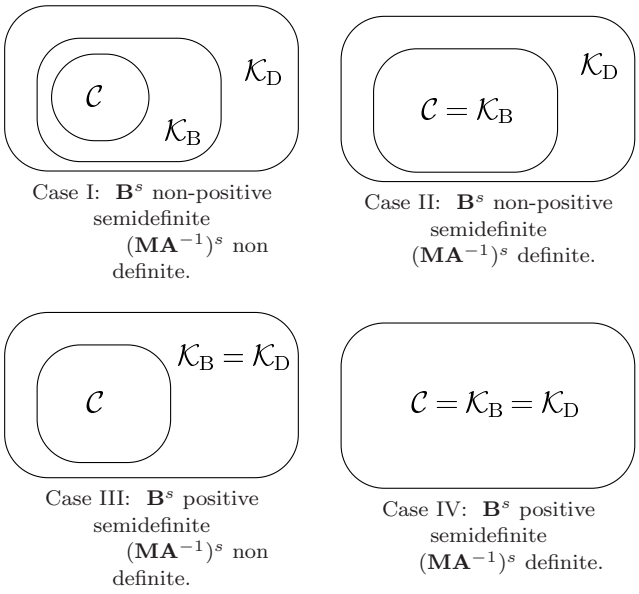

Fig. 1 *Relations among $\mathcal{C}, \mathcal{K}_{\mathrm{B}}$ and $\mathcal{K}_{\mathrm{D}}$*

3. The most interesting case is when the projected velocity $\dot{\mathbf{q}}$ does not belong to any kernel; that is, the projected velocity is incompatible and $\dot{\mathbf{q}} \notin \mathcal{K}_{\mathrm{D}}$, which means that some artificial energy is introduced ($\Delta E_p \neq 0$).
   In this situation, the second term ΔE_{p_2} of the projection energy given by (21) is always negative, since $\dot{\mathbf{q}} \notin \mathcal{K}_B$ and $\mathbf{M}^{-1}$ is a positive definite matrix, hence:

   $$\Delta E_{p_2} = -\frac{1}{2}\alpha^2\,(\mathbf{B}\dot{\mathbf{q}})^{\mathrm{T}}\,\mathbf{M}^{-1}\,(\mathbf{B}\dot{\mathbf{q}}) < 0$$

   However, the sign of the first term ΔE_{p_1} depends on the definiteness properties of matrix $\mathbf{B}^s$:
   (a) If $\mathbf{B}^s$ is non-positive semidefinite, ΔE_{p_1} may have any sign:

   $$\Delta E_{p_1} = -\alpha\dot{\mathbf{q}}^{\mathrm{T}}\mathbf{B}^s\dot{\mathbf{q}} \lesseqgtr 0 \quad .$$

   That means that the projection may dissipate or increase the energy of the system:

   $$\Delta E_p = \Delta E_{p_1} + \Delta E_{p_2} \lesseqgtr 0 \quad .$$

   (b) If $\mathbf{B}^s$ is positive semidefinite, (Cases III and IV), the first energy term is given by:

   $$\Delta E_{p_1} = -\alpha\dot{\mathbf{q}}^{\mathrm{T}}\mathbf{B}^s\dot{\mathbf{q}} \leq 0 \quad ,$$

   which means that the projection dissipates energy:

   $$\Delta E_p = \Delta E_{p_1} + \Delta E_{p_2} < 0 \quad .$$

Based on the previous results, it is clear that it is desirable to select a projection matrix $\mathbf{A}$ in which $\mathbf{B}^s$ is positive semidefinite, as in Cases III and IV. With this choice, no energy growth can ever be introduced by the projection. The difference between Cases III and IV is that Case III may leave incompatible velocities undamped ($\dot{\mathbf{q}} \notin \mathcal{C}, \dot{\mathbf{q}} \in \mathcal{K}_{\mathrm{D}}$), while Case IV always guarantees damping for any incompatible velocity.

The next proposition justifies the positive performance of projections based on the mass matrix $\mathbf{M}$:

Proposition 6 *A velocity projection performed with the mass matrix ($\mathbf{A} = \mathbf{M}$) introduces non-negative energy dissipation.*

We are immediately able to prove this based on the previous results, because in this case:

$$\mathbf{B} = \mathbf{M}\mathbf{A}^{-1}\mathbf{\Phi}_{\mathbf{q}}^{\mathrm{T}}\mathbf{\Phi}_{\mathbf{q}} = \mathbf{\Phi}_{\mathbf{q}}^{\mathrm{T}}\mathbf{\Phi}_{\mathbf{q}}$$

is always a symmetric and positive semidefinite matrix. Additionally, in this case $(\mathbf{M}\mathbf{A}^{-1})^s = \mathbf{1}$, which is a definite matrix. This situation corresponds to Case IV of Figure 1, where all incompatible velocities introduce dissipation, $\Delta E_p < 0$. □

Next, a numerical experiment is presented in order to verify the theoretical results outlined in the previous sections.

6 Numerical experiment

Let us consider a mechanical system composed of two particles with masses $m_1 = 1$ and $m_2 = \mu > 0$ moving along a smooth horizontal line, as depicted in Figure 2. The configuration of the system is defined by the vector of coordinates $\mathbf{q} = (q_1, q_2)^{\mathrm{T}}$ containing the distances of the particles from a fixed point on the line. In addition, there is a holonomic constraint $\Phi(\mathbf{q}) = \mathbf{q}^{\mathrm{T}}\mathbf{q} - 1 = q_1^2 + q_2^2 - 1 = 0$, and as a consequence the system has only one degree of freedom. The motion starts at $t = 0$ from

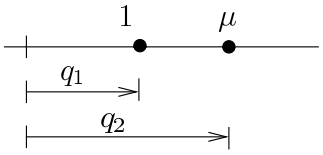

Fig. 2 *Two-particle example*

position $\mathbf{q}_0 = (0, 1)^{\mathrm{T}}$ with velocity $\dot{\mathbf{q}}_0 = (1, 0)^{\mathrm{T}}$. Taking into account that $\Phi_{\mathbf{q}} = 2\mathbf{q}$, it is easy to verify that the constraints at position and velocity levels are satisfied at $t = 0$:

$$\Phi_0 = \mathbf{q}_0^{\mathrm{T}}\mathbf{q}_0 - 1 = 0 \quad , \quad \dot{\Phi}_0 = \Phi_{\mathbf{q}}^{\mathrm{T}}\dot{\mathbf{q}}_0 = 2(0,1)\cdot(1,0)^{\mathrm{T}} = 0$$

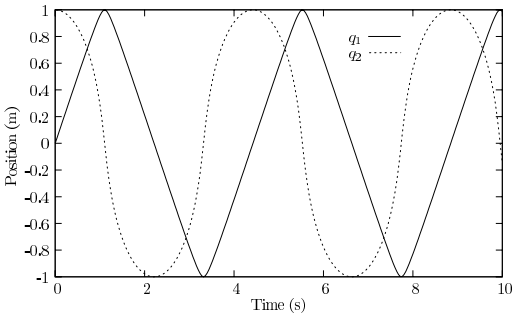

Fig. 3 Position vs. time. Conserving integration without projections, $\Delta t = 0.04$ s

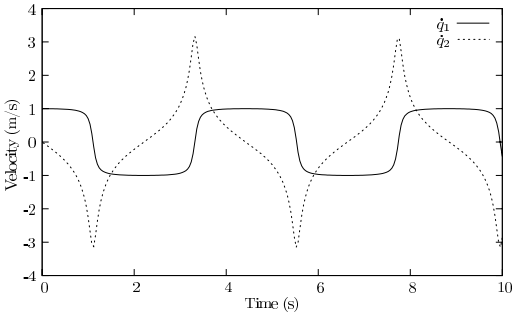

Fig. 4 Velocity vs. time. Conserving integration without projections, $\Delta t = 0.04$ s

The motion is integrated up to 10 s with a conserving augmented Lagrangian scheme in position with a penalty of 10^3 (see [17] for details of the formulation), such that the constraint at position level is exactly satisfied with exact energy conservation, $\Delta E_i = 0$, as expressed in section 4 with expression (14). No projections are performed.

Figures 3 and 4 show, respectively, the evolution of the position $\mathbf{q}$ and velocity $\dot{\mathbf{q}}$ in time for $\mu = 0.1$ with a constant time step $\Delta t = 0.04$ s. Figure 5 shows the discrete energy, which is exactly constant, as expected, and Figure 6 shows the Lagrange multiplier, which is related to the constraint force by $\mathbf{Q}_{\Phi} = \Phi_{\mathbf{q}}^{\mathrm{T}}\lambda = 2\lambda\mathbf{q}$.

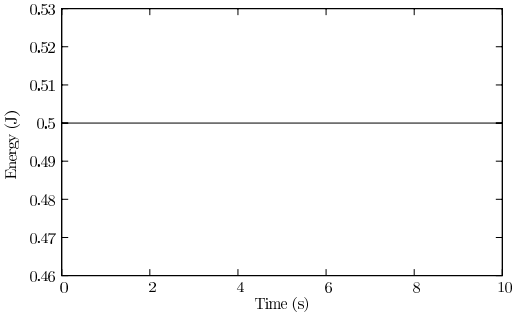

Fig. 5 Energy vs. time. Conserving integration without projections, $\Delta t = 0.04$ s

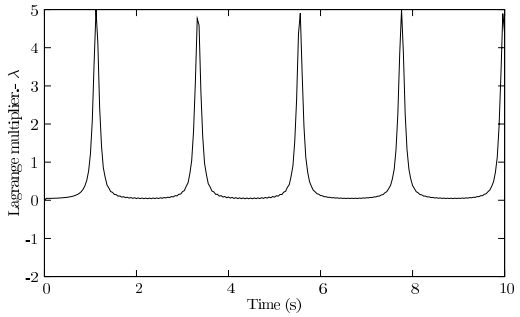

Fig. 6 Lagrange multiplier vs. time. Conserving integration without projections, $\Delta t = 0.04$ s

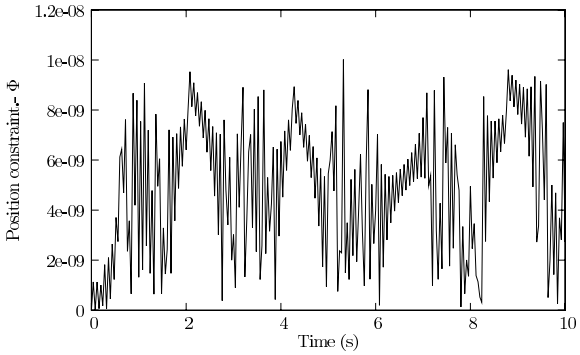

Fig. 7 Position constraint vs. time. Conserving integration without projections, $\Delta t = 0.04$ s

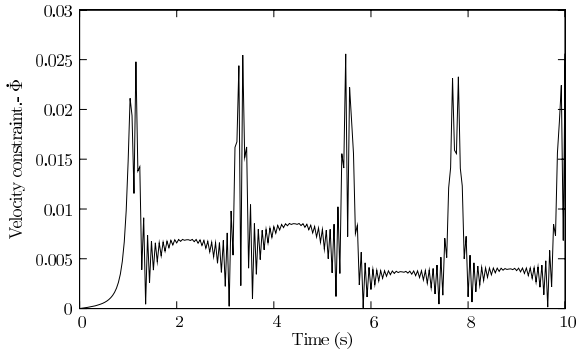

Fig. 8 Velocity constraint vs. time. Conserving integration without projections, $\Delta t = 0.04$ s

Figures 7 and 8 show the constraints at position and velocity levels. It is possible to observe in Figure 7 that the position constraint remains small ($\simeq 10^{-9}$), but Figure 8 shows that the velocity constraint is much larger ($\simeq 10^{-2}$), as expected since no projections are performed. Nevertheless, the energy control performed by the integrator seems capable of handling this undesirable effect, avoiding a noticeable increase in the velocity constraint violation during the integration.

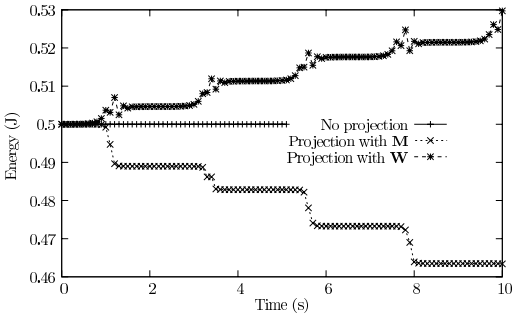

Fig. 9 Energy vs. time. Conserving integration, $\Delta t = 0.1$ s

A second set of experiments is performed next, using a larger time integration step $\Delta t = 0.1$ s. As shown in Figure 9, the integration fails to converge at $t = 5.2$ s when no projections are performed, despite energy being exactly conserved.

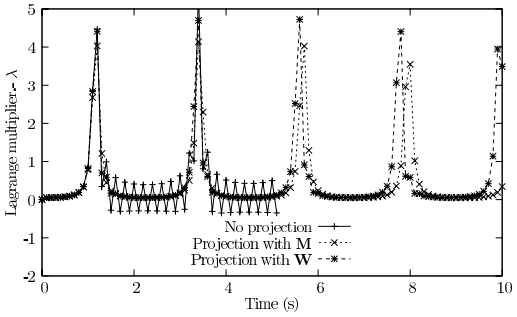

Fig. 10 Lagrange multiplier vs. time. Conserving integration, $\Delta t = 0.1$ s

Figure 10 shows that the instability at the end of the integration is related to the large oscillations on the Lagrange multiplier. Figure 11 shows that the position constraint is satisfied up to the failure, as expected, but the violation of the velocity constraint shown in Figure 12 is larger and exhibits a growing trend. Thus, it is reasonable to conclude that the growth of the velocity constraint violation is the ultimate cause of the instability that produces the ultimate failure of the integration.

If a velocity projection with (2) and (4) is performed, the velocity constraint may be significantly reduced and the integration may be carried up to $t = 10$ s, but the result depends on the projection matrix $\mathbf{A}$ employed.

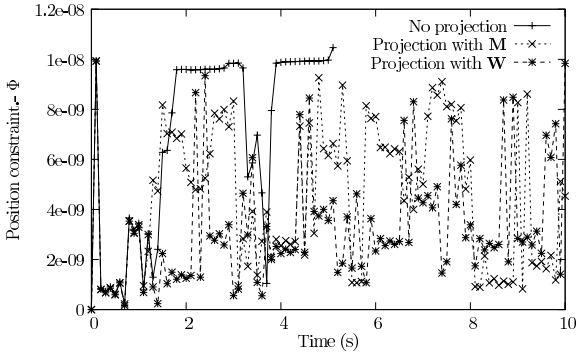

Fig. 11 Position constraint vs. time. Conserving integration, $\Delta t = 0.1$ s

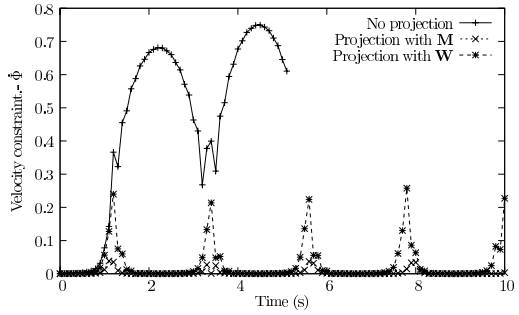

Fig. 12 Velocity constraint vs. time. Conserving integration, $\Delta t = 0.1$ s

Two matrices are tested: the mass matrix $\mathbf{A} = \mathbf{M} = \begin{pmatrix} 1 & 0 \\ 0 & \mu \end{pmatrix}$ with $\mu = 0.1$ and a positive definite matrix $\mathbf{A} = \mathbf{W}$ of the form:

$$\mathbf{W} = \begin{pmatrix} a & 0 \\ 0 & 1 \end{pmatrix} \qquad \text{with} \quad a > 0 \quad ,$$

with $a = 15$ and a projection penalty parameter $\alpha = 1$. This penalty parameter is far too small for practical simulations, but it will serve to more clearly show the performance of the projection technique.

Figures 11 and 12 show that, as expected, both projection matrices accomplish the task of reducing the velocity constraint, and they also stabilize the integration such that it may be carried up to the end time. But Figure 9 shows that there are important differences in the behaviour of the energy: while $\mathbf{M}$ avoids the growth of energy (as predicted in Proposition 6), matrix $\mathbf{W}$ causes an artificial growth of energy. This behaviour is justified by the properties of matrix $\mathbf{B}^s$, which are in this case:

$$\mathbf{B} = \mathbf{M}\mathbf{W}^{-1}\Phi_{\mathbf{q}}^{\mathrm{T}}\Phi_{\mathbf{q}} = 4\begin{pmatrix} q_1^2/a & q_1q_2/a \\ \mu q_1 q_2 & \mu q_2^2 \end{pmatrix}$$

$$\mathbf{B}^s = \frac{1}{2}\left(\mathbf{B} + \mathbf{B}^{\mathrm{T}}\right) = 2\begin{pmatrix} 2q_1^2/a & q_1q_2(\mu + 1/a) \\ q_1q_2(\mu + 1/a) & 2\mu q_2^2 \end{pmatrix}$$

It can be shown that matrix $\mathbf{B}^s$ is not positive semidefinite, because its determinant is:

$$\det(\mathbf{B}^s) = 4\left(\frac{4\mu}{a}q_1^2q_2^2\right) - q_1^2q_2^2\left(\mu + \frac{1}{a}\right)^2 = -\frac{4}{a^2}q_1^2q_2^2\left(1 - a\mu\right)^2 \leq 0$$

According to the conclusions presented at the end of section 5, this means that the energy may increase or decrease, which is in fact the behaviour shown in Figure 9.

Looking more closely at the projection performed with matrix $\mathbf{W}$, a quick inspection of matrix $\mathbf{M}\mathbf{W}^{-1}$ reveals that it is definite:

$$\mathbf{M}\mathbf{W}^{-1} = \begin{pmatrix} 1/a & 0 \\ 0 & \mu \end{pmatrix} \quad ,$$

which means that there could be incompatible velocities $\dot{\mathbf{q}}$ associated with a projection that does not modify the energy ($\Delta E_p = 0$), corresponding to Case II of Figure 1, with $\mathcal{C} = \mathcal{K}_B \subset \mathcal{K}_D$.

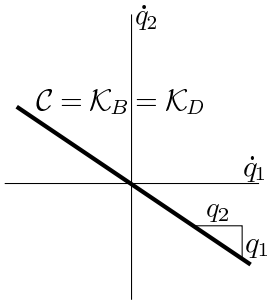

(a) $\mathbf{A} = \mathbf{M}$

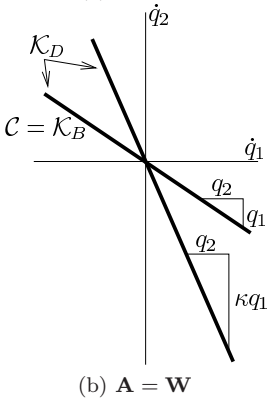

(b) $\mathbf{A} = \mathbf{W}$

Fig. 13 Kernels for projection matrices $\mathbf{A} = \mathbf{M}$ and $\mathbf{A} = \mathbf{W}$

The kernels $\mathcal{C}, \mathcal{K}_B$ and $\mathcal{K}_D$ for the particular case of matrices $\mathbf{A} = \mathbf{M}$ and $\mathbf{A} = \mathbf{W}$ can be obtained after some algebra using expressions (19), (20), (22), (23) and (24), and are depicted at Figure 13. In all cases the kernels are straight lines in $\mathbb{R}^2$, with a slope which depends on the configuration (q_1, q_2).

In the case of $\mathbf{A} = \mathbf{M}$ the three kernels collapse in a single straight line with slope $-q_1/q_2$, as shown in Figure 13 (a). This results totally agree with Proposition 6, based on the properties of matrices $\mathbf{B}^s = \mathbf{\Phi}_\mathbf{q}^\mathrm{T}\mathbf{\Phi}_\mathbf{q}$ and $\mathbf{M}\mathbf{A}^{-1} = \mathbf{1}$, corresponding to Case IV of Figure 1.

In the case of $\mathbf{A} = \mathbf{W}$, the kernel $\mathcal{K}_D$ consists of two lines with slopes $-q_1/q_2$ and $-\kappa q_1/q_2$, respectively, with $\kappa = (a + 2q_1^2 + 2a^2\mu^3 q_2^2)/(\mu a^2 + 2q_1^2 + 2a^2\mu^3 q_2^2)$, as shown in Figure 13 (b). Additionally, the kernels $\mathcal{C}$ and $\mathcal{K}_B$ collapse in a straight line with slope $-q_1/q_2$. Again, these results totally agree with the predictions made in previous paragraphs based on the properties of matrices $\mathbf{B}^s$ and $\mathbf{M}\mathbf{W}^{-1}$, corresponding to Case II of Figure 1.

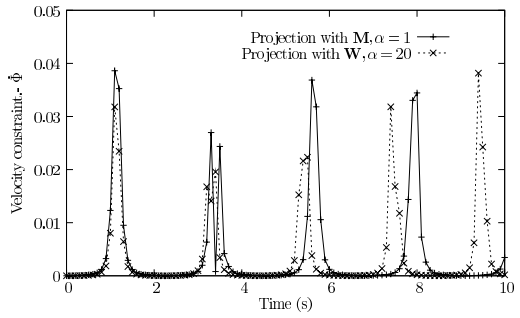

Fig. 14 Velocity constraint vs. time. Conserving integration with projections, $\Delta t = 0.1$ s

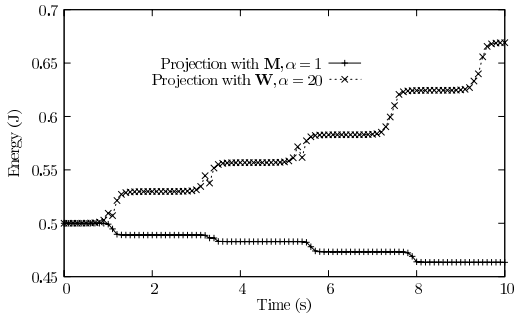

Fig. 15 Energy vs. time. Conserving integration with projections, $\Delta t = 0.1$ s

Finally, in order to study the effect of the penalty parameter α in relation to the projection energy balance, a new experiment is performed with the same projection matrix $\mathbf{W}$ and a larger projection penalty parameter, $\alpha = 20$. As shown in Figures 14 and 15, the larger penalty causes a significant reduction in the velocity constraint to the same order of magnitude as the values obtained with the mass matrix $\mathbf{M}$ combined

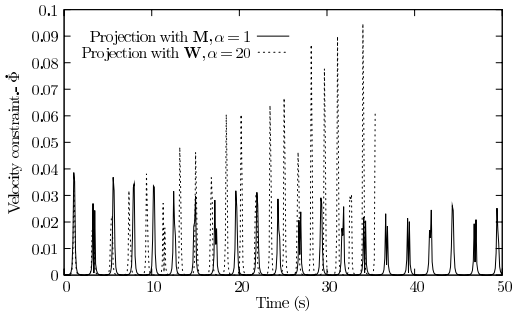

Fig. 16 Velocity constraint vs. time. Conserving integration with projections, $\Delta t = 0.1$ s

with a penalty $\alpha = 1$. However, it also can be observed, by comparing Figures 9 and 15, that the artificial energy added to the system increases significantly. While the energy at the end of the computation for $\alpha = 1$ is $E_{t=10} \simeq 0.53$ J (as shown in Figure 9), the energy for $\alpha = 20$ shown in Figure 15 is $E_{t=10} \simeq 0.67$ J.

Figure 16 shows the behaviour of the velocity constraint $\dot{\Phi}$ in a longer simulation, up to 50 s. The projection with $\mathbf{M}$ and $\alpha = 1$ retains a small violation of the velocity constraint, producing a stable integration although introducing significant dissipation ($E_{t=50}/E_{t=0} \simeq 0.74$). On the other hand, the projection with $\mathbf{W}$ and $\alpha = 20$ controls the violation of the constraint fairly well at the begining of the simulation; but it fails to keep it small, with integration failure occurring at $t = 35.5$ s. The large amount of energy introduced by the projection ($E_{t=35.5}/E_{t=0} \simeq 2.54$) is responsible for the growth of the velocity constraint's violation and the ultimate failure of the computation.

7 Conclusions

The main conclusions that may be drawn from the developments presented in this work are:

- A velocity projection, solving a minimization problem based on a positive definite matrix and using a penalty method, succeeds in maintaining the numerical solution of the index-3 DAE system close to the velocity constraint manifold $\dot{\mathbf{\Phi}} = \mathbf{0}$. This projection has a stabilization effect that has been reported in the literature and tested with a simple example in this paper.
- The velocity projection may introduce some artificial energy into the system. If this energy is negative (dissipation) the stabilization effect of the projections is enhanced, making it possible to adopt larger integration time steps or allowing longer term computations.

  On the other hand, a positive energy spoils the stabilization effect introduced by the projections, re-

sulting in an unrealistic motion and eventually a failure of the computations.
- The consequence of the previous statement is that not all positive definite matrices are suited to performing a useful projection. Some positive artificial energy may be introduced into the system, compromising the stability of the numerical scheme. The numerical experiment presented in this paper, despite its simplicity, shows this effect very clearly.
- For a system with a mass matrix $\mathbf{M}$, subject to a holonomic constraint function vector $\mathbf{\Phi}(\mathbf{q})$, a velocity projection does not increase the energy of the system if the symmetric part of the matrix $\mathbf{M}\mathbf{A}^{-1}\mathbf{\Phi}_\mathbf{q}^{\mathrm{T}}\mathbf{\Phi}_\mathbf{q}$ is positive semidefinite, $\mathbf{A}$ being the projection matrix.
  This property provides a practical criterion for the selection of a projection matrix, which is an important issue that is not explicitly discussed in the literature in this field.
- Additionally, if the symmetric part of the matrix $\mathbf{M}\mathbf{A}^{-1}$ is definite, the projection of incompatible velocities always introduces energy dissipation.
- Finally, the energy balance of the velocity projection provides an alternative justification for the positive performance of the mass-orthogonal projection reported in the literature.

Acknowledgements The author wishes to acknowledge the financial support of the Spanish Ministry of Science and Innovation as part of project DPI-2006-15613-C03-02 under the name "Modelización numérica eficiente de grandes sistemas flexibles con aplicaciones de impacto". The author would also like to thank Daniel Dopico (Universidad de La Coruña) and Ignacio Romero (Universidad Politécnica de Madrid) for their helpful comments.

References

1. T. Alishenas and Ö. Ólafsson. Modeling and velocity stabilization of constrained mechanical systems. *BIT Numerical Mathematics*, 34:455–483, 1994.
2. Martin Arnold and Olivier Bruls. Convergence of the generalized-alpha scheme for constrained mechanical systems. *Multibody System Dynamics*, 18:185–202, 2007.
3. Uri M. Ascher. Stabilization of invariants of discretized differential systems. *Numerical Algorithms*, 14:1–23, 1997.
4. Uri M. Ascher, Hongshenh Chin, Linda R. Petzold, and Sebastian Reich. Stabilization of constrained mechanical systems with daes and invariant manifolds. *Journal of Mechanics of Structures and Machines*, 23:135–158, 1995.
5. Uri M. Ascher and Linda R. Petzold. *Computer Methods for Ordinary Differential Equations and Differential-Algebraic Equations*. SIAM, 1998.
6. Olivier A. Bauchau and André Laulusa. Review of contemporary approaches for constraint enforcement in multibody systems. *Journal of Computational and Nonlinear Dynamics (ASME)*, 3:1–8, 2008.
7. E. Bayo and R. Ledesma. Augmented lagrangian and mass-orthogonal projection methods for constrained multibody dynamics. *Nonlinear Dynamics*, 9:113–130, 1996.
8. K. E. Brenan, S. L. Campbell, and L. R. Petzold. *Numerical Solution of Initial-Value Problems in Differential-Algebraic Numerical Solution of Initial-Value Problems in Differential-Algebraic Equations*. SIAM, 1996.
9. J. Cuadrado, J. Cardenal, and E. Bayo. Modeling and solution methods for efficient real-time simulation of multibody dynamics. *Multibody System Dynamics*, 1:259–280, 1997.
10. J. Cuadrado, J. Cardenal, P. Morer, and E. Bayo. Intelligent simulation of multibody dynamics: space-state and descriptor methods in sequential and pararell computing environments. *Multibody System Dynamics*, 4:55–73, 2000.
11. J. Cuadrado, D. Dopico, M.A. Naya, and M. González. Penalty, semi-recursive and hybrid methods for mbs real-time dynamics in the context of structural integrators. *Multibody System Dynamics*, 12:117–132, 2004.
12. E. Eich, C. Führer, B. Leimkhuler, and S. Reich. Stabilization and projection methods for multibody dynamics. Technical Report A281, Helsinki Institute of Technology, 1990.
13. Edda Eich. Convergence results for a coordinate projection method applied to mechanical systems with algebraic constraints. *SIAM Journal on Numerical Analysis*, 30(5):1467–1482, 1993.
14. J. C. García Orden and J. M. Goicolea. Conserving properties in constrained dynamics of flexible multibody systems. *Multibody System Dynamics*, 4:225–244, 2000.
15. J. C. García Orden and J. M. Goicolea. *Advances in Computational Multibody Dynamics.*, chapter Robust analysis of flexible multibody systems and joint clearances in an energy conserving framework, pages 205–237. Computational Methods in Applied Sciences. Springer-Verlag, 2005.
16. J.C. García Orden and D. Dopico Dopico. *Multibody Dynamics. Computational Methods and Applications*, chapter On the stabilizing properties of energy-momentum integrators and coordinate projections for constrained mechanical systems, pages 49–67. Computational Methods in Applied Sciences. Springer-Verlag, 2007.
17. J.C. García Orden and R. Ortega. A conservative augmented lagrangian algorithm for the dynamics of constrained mechanical systems. *Mechanics Based Design of Structures and Machines*, 34(4):449–468, 2006.
18. J. M. Goicolea and J. C. García Orden. Quadratic and higher-order constraints in energy-conserving formulations in flexible multibody systems. *Multibody System Dynamics*, 7:3–29, 2002.
19. Oscar González. Mechanical systems subjected to holonomic constraints: Differential-algebraic formulations and conservative integration. *Physica D*, 132:165–174, 1999.
20. E. Hairer and G. Wanner. *Solving Ordinary Differential Equations II, Stiff and Differential-Algebraic Problems*. Springer-Verlag, 1991.
21. T.R.J. Hughes. *The Finite Element Method*. Prentice Hall, 1987.
22. Ch. Lubich. Extrapolation integrators for constrained multibody systems. *Impact of Computing in Science and Engineering*, 3:213–234, 1991.
23. M. Ortiz. A note on energy conservation and stability of nonlinear time-stepping algorithms. *Computers and Structures*, 24(1), 1986.
24. A.M. Stuart and A.R. Humphries. *Dynamical Systems and Numerical Analysis*. Cambridge, 1996.